IEEE Sensors Council

MCDP: Maximizing Cooperative Detection Probability for Barrier Coverage in Rechargeable Wireless Sensor Networks

Pei Xu, Jianguo Wu, Chih-Yung Chang, *Member, IEEE*, Cuijuan Shang, and Diptendu Sinha Roy

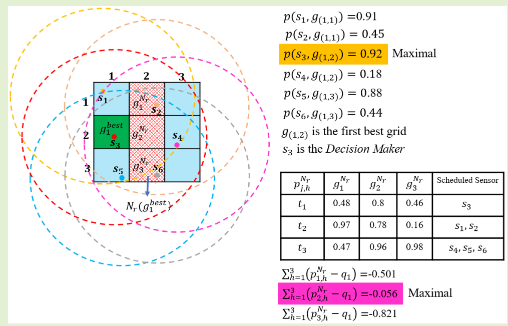

***Abstract*—Barrier coverage problem is an important issue in wireless sensor networks (WSNs). Many solutions have been proposed for constructing a defense barrier aiming to maximize the surveillance quality while prolonging the network lifetime. However, most of them assumed that the sensor nodes are battery powered without considering the rechargeable sensors. Though the energy conservation issue has been taken into account in most studies, the perpetual network lifetime is still impossible. In addition, most of existing works considered Boolean Sensing Model (BSM) which cannot reflect the physical features of sensing. This paper proposes a barrier coverage algorithm, called *MCDP*, which considers the rechargeable solar-powered sensors and applies the Probability Sensing Model (PSM) aiming to maximize the surveillance quality while the perpetual network lifetime of WSNs can be achieved. The *MCDP* algorithm first partitions the time line and monitoring region into several space time points and calculates the detection probability of each sensor to each space time point. Then the proposed *MCDP* algorithm schedules sensors staying in sensing state and recharging state in each time slot such that the weakest cooperative surveillance quality of the time-space point can be maximized. Experimental study shows that the proposed *MCDP* algorithm achieves better performance than existing work in terms of surveillance quality, stability of cooperative detection probability as well as fault tolerance.**

***Index Terms*—Barrier coverage, solar-powered sensor, probability sensing model, wireless sensor networks.**

I. Introduction

WIRELESS sensor networks have been applied to a wide range of applications including earthquake detection and prediction, environment monitoring, intruder detection in the hazardous region and so on. Network coverage is one of the most important issues in WSNs [1], which can be classified into three categories: target coverage, area coverage, and barrier coverage [2]. The target coverage aims to monitor some specific objects [3] such as museum and campus while the area coverage aims to monitor a given region [4] such as agricultural test field and chemical plant. Unlike target and area coverages, the barrier coverage aims to detect illegal intruders crossing a given region, which is mainly applied in border surveillance [5]. The barrier coverage problem has been widely discussed in the literature. The main challenge of the barrier coverage is the limited sensing ability and limited battery. Consequently, achieving the high surveillance quality while maintaining a long network lifetime has been the common goal of existing researches [6]–[8].

The surveillance quality of the barrier is generally determined by the sensing model and the barrier construction algorithm. Most of the existing approaches designed barrier construction algorithms based on the Boolean Sensing Model (BSM) which aimed to construct a barrier that satisfies k-barrier coverage [9]. The BSM assumes that the sensing ability of each sensor is perfect and the event occurred in the sensing range of each sensor is definitely detected. Under this assumption, the BSM is unable to reflect the physical features of sensing. Different from BSM, the Probability Sensing Model (PSM) describes the sensing ability by detection probability [19]. The algorithms based on PSM addressed barrier coverage problem and aimed to detect event with a

Manuscript received February 26, 2020; revised June 21, 2020; accepted December 6, 2020. Date of publication December 9, 2020; date of current version February 5, 2021. The associate editor coordinating the review of this article and approving it for publication was Prof. Henry Leung. *(Corresponding author: Chih-Yung Chang.)*

Pei Xu and Jianguo Wu are with the School of Computer Science and Technology, Anhui University, Hefei 230601, China (e-mail: xupeimk@163.com; wjg5408@163.com).

Chih-Yung Chang is with the Department of Computer Science and Information Engineering, Tamkang University, New Taipei 25137, Taiwan (e-mail: cychang@mail.tku.edu.tw).

Cuijuan Shang is with the School of Computer and Information Engineering, Chuzhou University, Chuzhou 239000, China (e-mail: shangcuijuan@chzu.edu.cn).

Diptendu Sinha Roy is with the Department of Computer Science and Engineering, National Institute of Technology Meghalaya, Shillong 793003, India (e-mail: diptendu.sr@nitm.ac.in).

Digital Object Identifier 10.1109/JSEN.2020.3043456

probability larger than the predefined requirement. The PSM is more practical as compared with BSM because it matches real sensing behavior.

The network lifetime is another challenge of barrier coverage problem [11]. Most of the previous studies assumed that the battery of sensor is energy constrained and developed energy management scheme to prolong the lifetime of the given wireless network [22]. They aimed to explore more distinct defense barriers, then designed the sleep-wake up algorithm based on the remaining energy of each sensor in order to balance the energy of each sensor. By applying this scheme, the network lifetime can be enhanced. However, the network lifetime is still limited. The deployed WSNs have to stop monitoring task and change the battery, which lead to a high cost. Some other studies considered the rechargeable solar-powered sensors which aimed to obtain a permanent lifetime. However, most of these researches cannot be applied in barrier coverage.

By applying the PSM, this paper addresses the barrier coverage problem and develops a barrier coverage construction algorithm, called maximizing cooperative detection probability or *MCDP* in short for wireless solar-powered sensor networks. In order to maximize the cooperative detection probability of the barrier, the *MCDP* algorithm first aims to identify the "bottleneck point" which has the weakest cooperative detection probability. Then *MCDP* algorithm prior allocates the sensor with the largest contribution to improve the cooperative detection probability of the bottleneck point. Then the *MCDP* algorithm schedules each sensor that participates in defense barrier to periodically recharge its battery while guaranteeing a certain level of surveillance quality.

The main contributions of the proposed *MCDP* algorithm are itemized as follows:

1) **The physical features of the sensor are taken into consideration.** Most existing works applied BSM to cope with the barrier coverage problem [12], [13]. The evaluation of sensing ability by applying BSM is not accurate, resulting in low surveillance quality or coverage holes in actual applications. This paper applies PSM to evaluate the sensing ability which can reflect the physical features of the sensing behavior.
2) **Weakest-first and contribution-based scheme for cooperative monitoring.** The proposed *MCDP* algorithm considers the cooperative detection probability and prior allocates the sensor with the largest contribution to monitor the bottleneck point. By applying this scheme, the surveillance quality of the constructed barrier can be significantly improved, as compared with the existing algorithms.
3) **Perpetuating the lifetime of the deployed WSNs.** The previous studies [14]–[16] aimed to prolong the network lifetime by reducing energy consumption. However, the battery-based sensor has an energy constraint in which its lifetime is still limited. This paper adopts the solar-powered sensor and designs a scheme for scheduling sensors to be recharged in turn such that the lifetime of deployed networks is perpetual.
4) **Make full use of all sensors.** The proposed *MCDP* algorithm aims to schedule all sensors to monitor the region periodically rather than selecting some sensors to construct a set of disjoint barriers. Therefore, surveillance quality can be significantly improved.

The rest of this paper is organized as follows. Section II presents the related work. Section III presents the network environment and problem statement. Section IV gives the details of the proposed *MCDP* algorithm. Section V further gives the simulation results. Finally, a conclusion of the proposed algorithm and future works are drawn.

II. Related Work

In literature, several barrier coverage algorithms have been proposed in recent years. In general, these studies are developed based on different sensing models and different assumptions on battery types. The following reviews these studies and compares them with our work.

A. Barrier Coverage by Applying BSM

A number of barrier coverage algorithms have been proposed by applying the BSM which assumed that the sensor has perfect sensing ability and can definitely detect the event that occurred in its sensing range. Yu *et al*. [9] first introduced a novel concept of coverage contribution area, aiming to reduce the redundancy of sensor selection for k-barrier coverage. Then two mechanisms are presented for solving the k-barrier coverage problem based on coverage contribution area. The constructed barriers satisfied k-barrier coverage with lower sensor spatial density. Weng *et al*. [14] presented a graph model, called CA-Net, which aims to simplify the problem of k-barrier coverage while reducing the computational complexity. Based on the developed CA-Net, a decentralized approach is presented to address the k-barrier coverage problem with the purposes of balanced energy and maximal lifetime. Silvestri *et al*. [17] proposed an autonomous deployed algorithm for k-barrier coverage with mobile sensor. This algorithm coordinated sensor movement in order to construct k distinct barriers. Kong *et al*. [18] proposed a software defined system consisting of the cloud-based architecture and a barrier maintenance algorithm. The proposed algorithm continuously retains the barrier coverage wrapping the dynamic zone. The above mentioned studies are developed based on the assumption that the BSM is applied. Since the sensing probability is practically changed with the distance between the sensor and the intruder, the performance estimations might not be accurate in real applications.

B. Barrier Coverage by Applying PSM

Different with the BSM, the PSM assumes that the sensing ability of each sensor is a probability value determined by the distance between the sensor and the intruder. Compared with the BSM, the PSM is more practical because it can reflect physical sensing behavior. Chang *et al*. [10] proposed two scheduling mechanisms which aim to achieve the predefined monitoring quality of traffic counting while satisfying the

TABLE I
COMPARISON OF THE MAIN CHARACTERISTICS OF THE PROPOSED *MCDP* WITH THE EXISTING RELATED WORKS

Related Work	Barrier Coverage	PSM	Rechargeable Battery	Perpetual Lifetime	Decentralized
[9]	✓	×	×	×	✓
[10]	✓	✓	×	×	×
[14]	✓	×	×	×	✓
[15]	✓	×	×	×	✓
[17]	✓	×	×	×	✓
[18]	✓	×	×	×	×
[20]	✓	✓	×	×	✓
[21]	✓	×	×	×	×
[22]	✓	×	×	×	✓
[23]	×	×	✓	✓	×
[24]	×	✓	✓	✓	×
[25]	×	×	✓	✓	×
MCDP	✓	✓	✓	✓	✓

minimum number of working sensors. Chen *et al*. [19] considered PSM and proposed an iterative scheme to provide strong barrier coverage, aiming to minimize the number of active sensors. Li *et al*. [20] applied PSM to analyze the detection probability of crossing path when the intruder crosses the barrier with the maximum moving speed. Though the above mentioned studies applied the PSM to develop the algorithms and aimed to improve the performance of surveillance quality, they did not consider the issue of energy management. To prolong the lifetime or even support the perpetual surveillance operations, some efforts are still required.

C. Barrier Coverage Aiming to Maximize the Network Lifetime

In literature, most of existing solutions for maximizing the network lifetime are developed under the assumption that sensors are battery powered. Chen *et al*. [11] developed a novel sleep-wake up algorithm for maximizing the network lifetime and proved that the algorithm guarantees barrier coverage and closed to the optimal solution in terms of the network lifetime. Kim *et al*. [15] considered the sensor network which is organized by a number of energy-scarce ground sensors with homogenous initial battery level and energy-plentiful mobile sensors. Then they proposed an efficient algorithm aiming to maximize the lifetime of barrier coverage. Gupta *et al*. [21] proposed a probabilistic approach to determine if a sensor in barrier is redundant. Then they proposed a scheduling protocol to schedule redundant sensors to stay in sleep state such that the energy consumption can be reduced. Zhang *et al*. [22] proposed a breach-free scheduling for barrier coverage in heterogeneous sensor networks. They proved that the problem of finding a lifetime-maximizing breach-free schedule is equivalent to the maximum node weighted path problem in a directed graph. Though studies fall in this category aimed to schedule the sensors for prolonging the network lifetime, the surveillance service cannot be continuously supported when the sensors in WSNs exhaust their energies.

D. Perpetual Network Lifetime for Wireless Sensor Networks

To support the perpetual lifetime of the barrier, some other studies considered that the rechargeable battery is mounted on the sensor, which can be recharged by an external energy source in order to prevent the energy exhaustion. Nelofar *et al*. [23] formulated a multi-objective optimization function to compute the optimal path for wireless charger and to construct intellectual routing for reducing energy consumption of sensor nodes in the renewable wireless sensor networks. Chen *et al*. [24] presented a reinforcement learning-based sleep scheduling for the solar-powered wireless sensor network with the goal of maximizing the area coverage. Ayadi *et al*. [25] proposed an enhanced sensor coverage with the Daubechies wavelet algorithm, aiming to identify the optimal position for each wireless charger such that the number of chargers to recharge all sensor nodes can be minimized. Although abovementioned studies have proposed the scheduling algorithms for a solar-powered WSN, the proposed algorithms cannot be applied to the barrier coverage.

Table I gives the comparison of the main characteristics of the proposed *MCDP* with the existing related works.

III. ASSUMPTIONS AND PROBLEM STATEMENT

This section firstly presents the network model and assumptions of the considered wireless solar-powered sensor networks. Then, the main features of the deployed sensor and the problem statements of this paper are introduced.

A. Network Model

This paper considers a rectangle region R with the size $L \times W$, where L and W are the length and width of R, respectively. Let B_{left}, B_{right}, B_{top} and B_{bottom} denote the left, right, top and bottom boundaries of R. A path is said to be a crossing path if it completely crosses from B_{bottom} to B_{top}. Let (x_v, y_v) represent the coordinates of a given point v in R. We assume that a set of n solar-powered sensors $S = \{s_1, s_2, \ldots, s_n\}$ have been randomly deployed in region R. Each sensor has a unique *ID* and is aware of its own location, remaining energy and the boundaries of R. Let (x_i, y_i) represent the coordinate of deployed sensor s_i. The sensing radius and communication radius of each sensor are denoted by r_s and r_c, respectively. In general, the communication radius is at least twice the sensing radius. That is $r_c \geq 2r_s$.

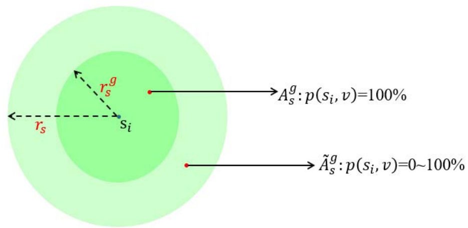

Fig. 1. The logic view of the probability sensing model.

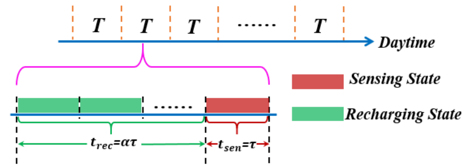

Fig. 2. An example of a cycle under condition $\sigma = \alpha + 1$.

B. Sensing Model

This paper applies the PSM (Probability Sensing Model). Fig. 1 depicts the main features of this model. The sensing range of any sensor s_i is divided into two regions. The inner region is the guaranteed sensing region and the outer region is the uncertain sensing region. Let $\mathcal{A}_s^g$ and $\tilde{\mathcal{A}}_s^g$ denote the guaranteed and uncertain sensing regions, respectively. The radius of the region $\mathcal{A}_s^g$ is r_s^g. If the event occurred in $\mathcal{A}_s^g$, the detection probability of sensor s_i to this event is 100%. However, in case that the event is occurred in $\tilde{\mathcal{A}}_s^g$, the detection probability of sensor s_i to this event will be decreased with the distance between the sensor s_i and the location of the occurred event which is ranging from 100% to 0%.

Let $p(s_i, v)$ denote the detection probability that sensor s_i detects an event occurred at the point v. Let $d(s_i, v)$ denote the distance between the sensor s_i and point v. The value of $p(s_i, v)$ can be calculated by applying the following expression.

$$p(s_i, v) = \begin{cases} 1 & d(s_i, v) \le r_s^g \\ e^{-\lambda\left(d(s_i, v) - r_s^g\right)^{\gamma}} & r_s^g < d(s_i, v) < r_s \\ 0 & d(s_i, v) \ge r_s \end{cases} \quad (1)$$

where λ and γ represent the path loss exponents of the sensing signal strength of the sensor and both two parameters can be adjusted with the physical properties of the sensor. The distance $d(s_i, v)$ in Exp. (1) can be obtained by applying the following expression.

$$d(s_i, v) = \sqrt{(x_i - x_v)^2 + (y_i - y_v)^2} \quad (2)$$

C. Recharging and Discharging Model

Assume that each solar-powered sensor is rechargeable. There are three possible states for each sensor: recharging state, sensing state and sleeping state. Each sensor consumes energy if it stays in sensing state which is called active sensor. A sensor stays in recharging state can be recharged from the solar energy when its power is not full. In case that the sensor stays in the sleeping state, it will do nothing while the remain energy of this sensor does not change.

Let τ denote the length of a time slot. Let recharging and discharging rates be the recharged energy and consumed energy of each sensor in each time slot, respectively. There are three physical parameters which impact the energy of each sensor, including battery capacity, discharging rate and recharging rate, which are denoted by E_{max}, u_{sen} and u_{rec}. Let E_{min} denote the minimal energy that required for maintaining the basic operation of each sensor. E_{min} is the threshold of energy below which the sensor cannot work and should switch to recharging state or sleeping state. Let t_{rec} denote the recharging time period which is the maximal time length required to fully recharge one sensor. Similarly, let t_{sen} denote the discharging time period which is the maximal time length that the sensor performs sensing task until its remaining energy equals to E_{min}. The value of t_{rec} and t_{sen} can be calculated by applying Exp. (3).

$$t_{rec} = \frac{E_{max} - E_{min}}{u_{rec}} \text{ and } t_{sen} = \frac{E_{max} - E_{min}}{u_{sen}} \quad (3)$$

Let α denote the ratio of the discharging and recharging rates. The value of α is

$$\alpha = \left\lceil \frac{u_{sen}}{u_{rec}} \right\rceil = \left\lceil \frac{t_{rec}}{t_{sen}} \right\rceil \quad (4)$$

The value of α is assumed to be an integer under the condition of $\alpha \ge 1$. The time line can be divided into several cycles, each cycle is denoted by T, which consists of σ equal-sized time slots, where $\sigma = \alpha + 1$. Fig. 2 shows an example of the time partition and a cycle T. Let $\tau = t_{sen}$ denote the length of each time slot. It is obvious that the value of t_{rec} is $\alpha\tau$ such that each sensor can be recharged energy for consuming in sensing state. Because that each sensor has the same schedule in each cycle, the developed algorithm only needs to cope with the scheduling of one cycle for each sensor.

D. Problem Statement

This paper considers the barrier coverage problem for a given wireless solar-powered sensor networks and proposes a barrier coverage algorithm, called *MCDP*. The proposed *MCDP* algorithm constructs a barrier which aims to maximize the surveillance quality while obtaining the perpetual lifetime of the deployed WSNs. The objective function and some constraints are presented as following.

Let ζ denote a possible scheduling algorithm. Let DB_ζ denote a constructed barrier based on ζ. Let t_h denote the h-th time slot in cycle T. Let $S_{v,h}^{act,\zeta}$ denote the set of active sensors which participate in DB_ζ at t_h and can cover point v. Recall that a path is said to be a crossing path if it completely crosses R from B_{bottom} to B_{top}. Recall that $p(s_i, v)$ denotes the detection probability that sensor s_i detect an event occurred at the point v. The probability that sensor s_i can't detect the event occurred at the point v is $1 - p(s_i, v)$. Consider a space time point (v, h), $v \in R$ and $h \in T$. The probability of all sensors $s_i \in S_{v,h}^{act,\zeta}$ cooperative monitor space time point (v, h) but unable to detect an occurred event is

$$\prod\nolimits_{s_i \in S_{v,h}^{act,\zeta}} (1 - p(s_i, v))$$

Let $p^{\zeta}_{\upsilon,h}$ denote the cooperative detection probability of all the sensors in $S^{act,\zeta}_{\upsilon,h}$ to (υ, h). The value of $p^{\zeta}_{\upsilon,h}$ can be calculated by applying Exp. (5).

$$p^{\zeta}_{\upsilon,h} = 1 - \prod\nolimits_{s_i \in S^{act,\zeta}_{\upsilon,h}} (1 - p(s_i, \upsilon)) \tag{5}$$

Let H denote the set of all the possible crossing paths. Let η_j denote the j-th crossing path in H. Let q^{ζ,η_j}_h denote the surveillance quality of DB_ζ to η_j at t_h. The q^{ζ,η_j}_h can be represented by the maximal cooperative detection probability of DB_ζ to any point on η_j at t_h. That is

$$q^{\zeta,\eta_j}_h = max_{\upsilon\in\eta_j}\ p^{\zeta}_{\upsilon,h} \tag{6}$$

Because there are different time slots in each cycle. In order to guarantee the surveillance quality of DB_ζ can be maximize at all time slots. The surveillance quality of DB_ζ to η_j, denoted by q^{ζ,η_j}, is the weakest surveillance quality at any time slot in one cycle. That is,

$$q^{\zeta,\eta_j} = min_{t_h\in T}\ q^{\zeta,\eta_j}_h \tag{7}$$

Let q^ζ denote the surveillance quality of DB_ζ. The q^ζ can be represented by the weakest surveillance quality of DB_ζ to all possible crossing paths. That is,

$$q^{\zeta} = min_{\eta_j\in H}\ q^{\zeta,\eta_j} \tag{8}$$

However, the number of points on η_j and the number of possible crossing paths are both infinite. This paper applies the grid-based approach to cope with this problem. The detail of this approach is presented in section IV.

The proposed *MCDP* algorithm aims to maximize the surveillance quality of the constructed barrier for detecting the intruder while maintaining the perpetual lifetime of the deployed solar-powered WSNs. The object function of this paper is given in Exp. (9).

Objective Function

$$Max(q^{\zeta} = min_{\eta_j\in H}\ q^{\zeta,\eta_j}) \tag{9}$$

Exp. (9) should be achieved under the condition that some constraints should be further satisfied. The following presents these constraints.

Let Boolean variables $M^{sen}_{j,h}$, $M^{rec}_{j,h}$ and $M^{slp}_{j,h}$ represent the sensing, recharging and sleeping states of sensor s_j at t_h, respectively. That is,

$$M^{sen}_{j,h} = \begin{cases} 1, & \text{if } s_j \text{ stays in sensing state at } t_h \\ 0, & \text{otherwise} \end{cases} \tag{10}$$

$$M^{rec}_{j,h} = \begin{cases} 1, & \text{if } s_j \text{ stays in recharging state at } t_h \\ 0, & \text{otherwise} \end{cases} \tag{11}$$

$$M^{slp}_{j,h} = \begin{cases} 1, & \text{if } s_j \text{ stays in sleeping state at } t_h \\ 0, & \text{otherwise} \end{cases} \tag{12}$$

It is obvious that each sensor can only stay in one state at any given time slot. Exp. (13) gives the constraint that each sensor can only stay in one of the three possible states at any given time.

(1) ***State Constraint***

$$M^{sen}_{j,h} + M^{rec}_{j,h} + M^{slp}_{j,h} = 1, \quad \forall j,\ \forall h \tag{13}$$

Let e_{rec} and e_{dis} denote the recharged and discharged capacity of each cycle, respectively, as shown in Exp. (14) and (15).

$$e_{rec} = \sum\nolimits_{h=1}^{\alpha+1} (M^{rec}_{j,h} \times u_{rec} \times \tau) \tag{14}$$

$$e_{dis} = \sum\nolimits_{h=1}^{\alpha+1} M^{sen}_{j,h} \times u_{sen} \times \tau \tag{15}$$

Exp. (16) gives the constraint that the total energies of recharging and discharging in each cycle T should be equal. This constraint guarantees the perpetual lifetime of each sensor.

(2) ***Perpetual Lifetime Constraint:***

$$\sum\nolimits_{h=1}^{\alpha+1} M^{sen}_{j,h} \times u_{sen} \times \tau = \sum\nolimits_{h=1}^{\alpha+1} (M^{rec}_{j,h} \times u_{rec} \times \tau) \tag{16}$$

Each scheduled sensor should be activated for only one time slot in each cycle. The following constraint shows this requirement.

(3) ***Sensing Time Constraint***

$$\sum\nolimits_{h}^{h+T} M^{sen}_{j,h} = 1, \quad \forall h \tag{17}$$

Some other constraint for the constructed barrier is that the set of active sensors whose sensing ranges can form a continuous barrier without containing any coverage hole. Let $\mathcal{A}_i$ denote the coverage area of sensor s_i. The following constraint shows that the coverage areas of two neighboring active sensors should be overlapped with each other in the constructed DB_ζ.

(4) ***Continuous Constraint:***

$$\mathcal{A}_i \cap \mathcal{A}_{i+1} \neq \emptyset, \quad \forall s_i \in DB_\zeta \tag{18}$$

Another important property that should be satisfied for a barrier is the boundary constraint. Let $s_{leftmost}$ and $s_{rightmost}$ denote the leftmost and rightmost sensors of the constructed DB_ζ, respectively. The boundary constraint requires that the coverage areas of $\mathrm{S}_{leftmost}$ and $\mathrm{S}_{rightmost}$ should be intersected with the B_{left} and B_{right}, respectively. The following gives the boundary constraint.

(5) ***Boundary constraint:***

$$\mathcal{A}_{leftmost} \cap B_{left} \neq \emptyset \wedge \mathcal{A}_{rightmost} \cap B_{right} \neq \emptyset,$$

where

$$s_{leftmost}, s_{rightmost} \in DB_\zeta \tag{19}$$

The next section presents the proposed *MCDP* algorithm which aims to achieve the objective function shown in Exp. (9) while satisfying constraints given in Exps. (13), (16), (17), (18) and (19).

IV. The Proposed MCDP Algorithm

The proposed algorithm, called Maximizing Cooperative Detection Probability (*MCDP*), aims to construct a defense barrier for a given solar-powered sensor network. The sensors perform sensing task and recharging task in turn such that the lifetime of each sensor can be perpetual. Besides, the proposed

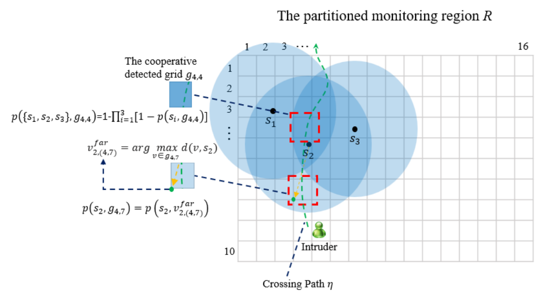

Fig. 3. The partitioned monitoring region R based on the grid-based method.

MCDP algorithm aims to schedule sensors working in an efficient way such that the cooperative monitoring can support maximal surveillance quality. The following presents the detail of the *MCDP* algorithm.

The *MCDP* algorithm mainly consists of three phases: *Space-Time Partitioning Phase*, *Computation Phase* and *Barrier Construction and Sensor Scheduling Phase*. The *Space-Time Partitioning Phase* initially partitions the monitoring region R into several equal-sized grids and the time line into several equal length time slots. The *Computation Phase* mainly defines the cycle length based on the ratio of recharging and discharging rates. Then the contribution of each sensor to each grid is calculated. Finally, the *Barrier Construction and Sensor Scheduling Phase* identifies the bottleneck point which is the space time point with the weakest detection probability. Finally, the sensor with the largest contribution to the bottleneck point will be selected as the active sensor, aiming to maximize the surveillance quality of the defense barrier while maintaining the perpetual network lifetime.

A. Space-Time Partitioning Phase

The main concept of this algorithm is to find the bottleneck space time points of all possible crossing paths and maximizes the detection probability of bottleneck space time point in each round. However, the number of possible crossing paths is infinite. This implies that the number of possible space time points is uncountable. In order to simplify the investigated issue and reduce computation complexity, the grid-based approach is adopted. In this phase, the monitoring region R is partitioned into $c_1 \times c_2$ equal-sized grids. The detection probabilities of one sensor to all the points in one grid are simply considered to be identical. Each grid will be labeled with two-dimensional coordinates. The most top-left grid in R is labeled with $(1, 1)$. The x-coordinate and y-coordinate are increased by one if the location of a grid shifts one position toward the right and down directions. Let $g_{(x,y)}$ denote the grid with coordinates (x, y). Fig. 3 shows an example of a monitoring region R, which is partitioned into 16×10 equal-sized grids. The sensors s_1, s_2 and s_3 are three active sensors for participating in a defense barrier.

Recall that the t_{rec} and $\alpha = \left\lceil \frac{u_{sen}}{u_{rec}} \right\rceil = \left\lceil \frac{t_{rec}}{t_{sen}} \right\rceil$ denote the recharging rate and the ratio of the discharging and recharging rate. According to the principle of energy balance, we have,

$$t_{rec} = \alpha\tau = \alpha \left\lceil \frac{E_{max} - E_{min}}{u_{sen}} \right\rceil \tag{20}$$

B. Computation Phase

This phase consists of two tasks: cycle length calculation and detection probability calculation. Since the schedule of each sensor is cycle-based, the first task aims to calculate the length of each cycle. Then the second task calculates the detection probability of each sensor.

Task I (Cycle Length Calculation): The proposed *MCDP* algorithm is a cycle-based scheduling scheme. That is, each sensor has the same schedule in each cycle. Each scheduled sensor only has two operations in one cycle: the sensing operation and the recharging operation. As mentioned above, each cycle consists of σ time slots. Each sensor should be fully recharged for supporting the sensing operations, aiming at maximizing the surveillance quality. Recall that each cycle is denoted by T. The length of T can be calculated by applying Exp. (21).

$$T = t_{sen} + t_{rec} = \alpha\tau + \tau \tag{21}$$

It is obvious that $\sigma = \alpha + 1$. That is, each sensor performs the sensing operation for one slot and then is recharged for α time slots.

Task II (Detection Probability Calculation): This task aims to calculate the detection probability of each sensor to each grid. Assume that sensor s_i can cover grid $g_{(x,y)}$. The detection probability depends on the situation whether or not the $g_{(x,y)}$ is fully covered by s_i. In case that a grid $g_{(x,y)}$ is not fully covered by the sensor s_i, the intruder can cross it through the uncovered space of this grid. Therefore, the detection probability of sensor s_i to $g_{(x,y)}$ is 0. On the contrary, if the sensor s_i can fully cover grid $g_{(x,y)}$, the detection probability of s_i to $g_{(x,y)}$ depends on the distance between s_i and $g_{(x,y)}$. Let $p\left(s_i, g_{(x,y)}\right)$ denote the detection probability of s_i to $g_{(x,y)}$. Let $v^{far}_{i,(x,y)}$ denote the farthest point in $g_{(x,y)}$ to s_i. That is,

$$v^{far}_{i,(x,y)} = arg \max_{v\in g(x,y)} d(v,s_i) \tag{22}$$

In order to guarantee the surveillance quality, the point $v^{far}_{i,(x,y)}$ is selected as the representative point of grid $g_{(x,y)}$. Therefore, the detection probability of s_i to $g_{(x,y)}$ can be calculated by applying Exp. (23)

$$p\left(s_i, g_{(x,y)}\right) = p\left(s_i, v^{far}_{i,(x,y)}\right) \tag{23}$$

The following further discusses the case that two or more active sensors can fully cover grid $g_{(x,y)}$. Let $\Phi_{(x,y)} = \{s^{act}_1, s^{act}_2, \ldots, s^{act}_f\}$ denote the set of active sensors that fully covers grid $g_{(x,y)}$. Let $p^{coop}\left(\Phi_{(x,y)}, g_{(x,y)}\right)$ denote the cooperative detection probability of all sensors in $\Phi_{(x,y)}$ to $g_{(x,y)}$. The value of $p\left(\Phi_{(x,y)}, g_{(x,y)}\right)$ can be calculated by applying Exp. (24)

$$p^{coop}\left(\Phi_{(x,y)}, g_{(x,y)}\right) = 1 - \prod_{k=1}^{f}\left[1 - p\left(s^{act}_k, g_{(x,y)}\right)\right] \tag{24}$$

As shown in Fig. 3, grid $g_{(2,7)}$ is not fully covered by sensor s_2, we have $p\left(s_2, g_{(2,7)}\right) = 0$. On the contrary, grid $g_{(4,7)}$ is fully covered by sensor s_2, the farthest point in $g_{(4,7)}$ to s_2 is marked by the green point as shown in Fig. 3.

The detection probability of s_2 to $g_{(4,7)}$ is determined by the distance between s_2 and $v^{far}_{2,(4,7)}$. By applying the sensing model presented in Exp. (1), we have,

$$\begin{aligned} & p\left(s_2, g_{(4,7)}\right) \\ & \quad = p\left(s_2, v^{far}_{2,(4,7)}\right) \\ & \quad = \begin{cases} 1 & d\left(s_2, v^{far}_{2,(4,7)}\right) \le r^g_s \\ e^{-\lambda\left(d\left(s_2, v^{far}_{2,(4,7)}\right) - r^g_s\right)^{\gamma}} & r^g_s < d\left(s_2, v^{far}_{2,(4,7)}\right) < r_s \\ 0 & d\left(s_2, v^{far}_{2,(4,7)}\right) \ge r_s \end{cases} \end{aligned}$$

Furthermore, grid $g_{(4,4)}$ is fully covered by sensors s_1, s_2 and s_3. That is, we have $\Phi_{(4,4)} = \{s_1, s_2, s_3\}$. The cooperative detection probability of s_1, s_2 and s_3 to $g_{(4,4)}$ is

$$p^{coop}\left(\Phi_{(4,4)}, g_{(4,4)}\right) = 1 - \prod_{k=1}^{3}\left[1 - p\left(s_k, g_{(4,4)}\right)\right]$$

Let $c_{i,(x,y)}$ denote the surveillance contribution of sensor s_i to grid $g_{(x,y)}$. The value of $c_{i,(x,y)}$ can be calculated by applying Exp. (25).

$$c_{i,(x,y)} = p^{coop}\left(\Phi_{(x,y)} \cup s_i, g_{(x,y)}\right) - p^{coop}\left(\Phi_{(x,y)}, g_{(x,y)}\right) \tag{25}$$

In this phase, the length of the cycle, the detection probability of each grid and the contribution of each sensor to each grid can be obtained. When *MCDP* algorithm finishes these computations, the next phase will construct the barrier by scheduling the sensors based on their contribution of detection probability to the bottlenecked space time point.

C. Barrier Construction and Sensor Scheduling Phase

This phase aims to schedule a set of active sensors working in different time slots for constructing a barrier, aiming to maximize the surveillance quality while lifetime of each sensor can be perpetuated. The main idea is to select the grid that obtains the maximal detection probability in each column of the partitioned region R as the best grid round by round from B_{left} to B_{right}. Then *MCDP* algorithm prior allocates the unscheduled sensor which has the largest contribution for improving the cooperative detection probability at the bottleneck space time point.

In the conceptual level, the *MCDP* algorithm initially divides all the sensors into several groups from B_{top} to B_{bottom}. Sensors in each group can form an independent defense barrier and thus several independent barriers can be constructed by different groups. To maximize the surveillance quality of each constructed defense barrier, sensors in each group will be scheduled from B_{left} to B_{right} based on their contributions in terms of detection probabilities. In each group, each unscheduled sensor first calculates their detection probability to each grid. Then the *MCDP* algorithm identifies the bottleneck space time point. Finally, the sensor that has the largest contribution to the bottleneck space time point will be scheduled to join the defense barrier.

Fig. 4 gives the flow chart of barrier construction and sensor scheduling phase. This phase mainly consists of five tasks. The first task divides all the sensors into some disjoint groups.

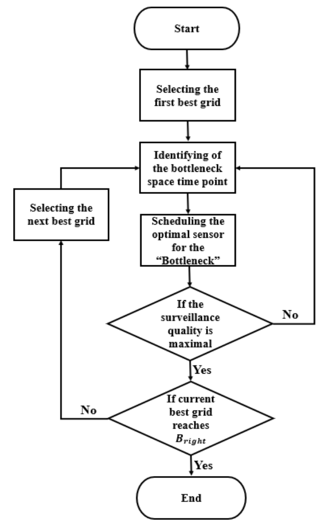

Fig. 4. The flow chart of barrier construction and sensor scheduling phase.

The second task selects the first best grid for initializing the barrier construction process in each group. The third task aims to identify the bottleneck space time point of the selected best grid. Then the fourth task selects one unscheduled sensor which has the largest contribution for improving the cooperative detection probability of the bottleneck space time point and schedules the selected sensor to join the defense barrier. The operations in the third and the fourth tasks will be repeatedly executed until the maximal surveillance quality of the bottleneck space time point has been achieved. The last task further selects the next best grid such that the barrier can be extended continuously. Then the operations of the third and fourth tasks will be performed again for the new selected grid. This phase will be terminated until the rightmost best grid reaches the right boundary and the surveillance quality of the rightmost best grid has been maximized.

Task I (Group Sensors Partitioning): This task aims to divide all the sensors into several groups. Sensors in different groups can form different independent barriers which can work together for supporting a higher surveillance quality. Fig. 5 gives an example of the partitioned groups. As shown in Fig. 5, the region R is partitioned into three sub-regions. The first, second and third sub-regions are the spaces consists of rows 1-3, rows 4-6 and rows 7-10, and are marked with blue, yellow and purple colors, respectively. Sensors fall in different sub-regions form different groups. The following illustrates how the proposed *MCDP* algorithm constructs one barrier for the first group. The constructions of other barriers are similar and will be omitted in this paper.

Tas II (Selecting the First Best Grid): This task aims to select the first best grid such that the barrier construction process can be initialized. Recall that each grid is labeled with two-dimensional coordinates (x, y). All sensors which can cover any grid $g_{(1,j)}$ should calculate its detection probability to $g_{(1,j)}$. The grid which has the maximal detection probability will be selected as the g^{best}_1.

Fig. 6 gives an example of selecting the first best grid. Assume that $S = \{s_1, s_2, s_3, s_4, s_5, s_6\}$ are the set of sensors

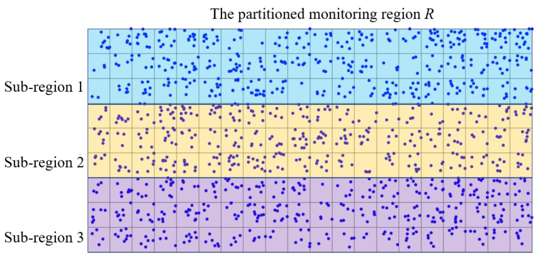

Fig. 5. An example of partitioned groups.

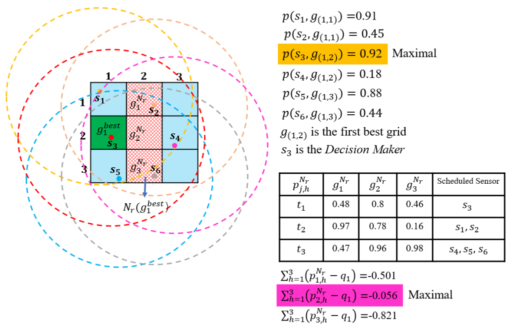

Fig. 6. An example of selecting the first best grid.

that can cover left boundary grids $g_{(1,1)}, g_{(1,2)}$ or $g_{(1,3)}$ in sub-region 1. Each sensor $s_i \in S$ calculates its detection probability to $g_{(1,1)}, g_{(1,2)}$ and $g_{(1,3)}$. By applying Exp. (23), the value of $p(s_3, g_{(1,2)})$ is maximal and is marked with yellow color. Therefore, grid $g_{(1,3)}$ is selected as the first best grid which is marked with green color.

When the g_1^{best} has been selected, the next two tasks aim to identify the bottleneck space time point of g_1^{best} and schedule the unscheduled sensor which has the largest detection probability contribution to the bottleneck space time point of g_1^{best}.

Task III (Identifying of the "Bottleneck Space Time Point"): This task aims to identify the bottleneck space time point of the newly selected best grid such that the cooperative detection probability can be maximized. Recall that the notation (v, h) represents a space time point. Recall that the detection probabilities of one sensor to all the points in one grid are considered to be identical. Let g_i^{best} with coordinates (x, y) be the selected best grid and (g_i^{best}, h) denote the considered space time point associated with grid g_i^{best} at time slot t_h. This task aims to identify the bottleneck time slot of grid g_i^{best}. Recall that each cycle T consists of σ time slots. Let S^{unsch} denote the set of unscheduled sensors. Let $S_{i,*}^{unsch}$ denote the set of sensors which can cover grid g_i^{best} but is unscheduled to any time slot. Let $S_{*,h}^{sch}$ denote the set of sensors which have been already scheduled to t_h. Let $S_{i,h}^{sch}$ denote the set of sensors which have been scheduled for monitoring g_i^{best} at time slot t_h. Let $p_{i,h}^{best}$ denote the cooperative detection probability of g_i^{best} at time slot t_h. By applying the Exps. (23) and (24), the value of $p_{i,h}^{best}$ is

$$p_{i,h}^{best} = 1 - \prod\nolimits_{s_j \in S_{i,h}^{sch}} \left(1 - p\left(s_j, g_i^{best}\right)\right) \tag{26}$$

Let t_i^{bott} denote bottleneck time slot of g_i^{best}, at which the cooperative detection probability of g_i^{best} is weakest in cycle T. That is,

$$t_i^{bott} = \arg \min_{1 \le t_h \le \sigma} p_{i,h}^{best} \tag{27}$$

In case that there are more than one time slots which satisfy Exp. (27), the earliest time slot will be treated as the bottleneck time slot.

Task IV (Scheduling the Sensor for the "Bottleneck"): This task aims to select the unscheduled sensors to improve the cooperative detection probability of the bottleneck space time point. Consider the best grid g_i^{best}. The following defines the Scheduling Matrix M which represents the scheduling result of this phase.

Definition (Scheduling Matrix of Best Grid g_i^{best}): A scheduling matrix of best grid g_i^{best}, denoted by $\mathcal{M}^{g_i^{best}}$, is a two-dimensional matrix with size $a \times \sigma$, where a denotes the number of sensors that cover grid g and σ denotes the number of time slots in each cycle. The value of $\mathcal{M}^{g_i^{best}}[i, j]$ is either '*sen*' or '*rec*', denoting that the sensor in i-th row, denoted by $\hat{s}_i$, stays in sensing or recharging states, respectively, at time slot t_j. That is,

$$\mathcal{M}^{g_i^{best}}[i, j] = \begin{cases} sen & if\ \hat{s}_i \text{ stays in sensing state} \\ rec & otherwise \end{cases}$$

□

Let *DM* denote the *Decision Maker* that is responsible for the scheduling operation. Let notation $\mathfrak{D}_i$ denote the *DM* node which is the closest sensor to the central point of the g_i^{best}. This task is performed repeatedly until all the sensors which have contribution to g_i^{best} have been scheduled. Let p_i^{bott} denote the cooperative detection probability at t_i^{bott}. Let s^{opt} denote the optimal sensor that has largest contribution to g_i^{best} at slot t_i^{bott}. Recall that $\Phi_{(x,y)}$ and $p^{coop}\left(\Phi_{(x,y)}, g_{(x,y)}\right)$ denote the set of active sensors that can fully cover grid $g_{(x,y)}$ and the cooperative detection probability of all sensors in $\Phi_{(x,y)}$ to $g_{(x,y)}$, respectively. We have,

$$s^{opt} = \arg \max_{s_j \in S_{i,*}^{unsuch}} \left[p^{coop}\left(\Phi_{\left(g_i^{best}\right)} \cup s_j, g_i^{best}\right) - p^{coop}\left(\Phi_{\left(g_i^{best}\right)}, g_i^{best}\right)\right] \tag{28}$$

Let S_i^{opt} denote the set of sensors that satisfy Exp. (28). In case that two more sensors satisfy Exp. (28), the *MCDP* algorithm will further check other advantages of each sensor in S_i^{opt}. In order to fully utilize sensors from top to bottom, the sensor which is located at the upper position will be prior selected as the s^{opt}. that is,

$$s^{opt} = arg \min_{s_j \in S_i^{opt}} y_j \tag{29}$$

where y_j is the y-coordinate of sensor s_j, as defined previously. The sensors which satisfy Exp. (29) can be retained in S_i^{opt}. If there are still more than one sensors in S_i^{opt}, the $\mathfrak{D}_i$ will randomly select one sensor in S_i^{opt} to play the role of s^{opt}.

As a result, the s^{opt} can be uniquely determined and should be removed from $S_{i,*}^{unsch}$. That is,

$$S_{i,*}^{unsch} = S_{i,*}^{unsch} \setminus \{s^{opt}\} \tag{30}$$

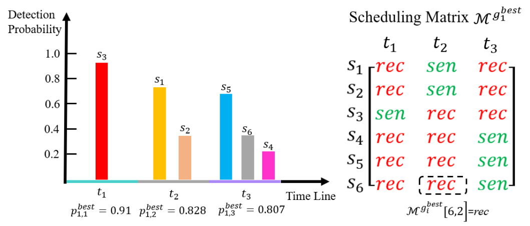

Fig. 7. The scheduling result of the example given in Fig. 6.

Then s^{opt} will be arranged to improve the detection probability of g_i^{best} at t_i^{bott}. The new bottleneck time slot should be reidentified by applying Exp. (27). Then the scheduling operations of the next round will be started to repeatedly find another s^{opt}. Let q_i denote the surveillance quality of g_i^{best} which is the weakest cooperative detection probability at any time slot of one cycle. That is

$$q_i = arg\,\underset{t_h \in T}{min}\; p_{i,h}^{best} \tag{31}$$

The scheduling operation for g_i^{best} will be terminated if q_i cannot be further improved.

To illustrate the operations designed in this phase, the following gives an example which continues the example shown in Fig. 6. Since $g_{(1,2)}$ is selected as g_1^{best} and s_3 is the closest sensor to the central point of $g_{(1,2)}$, s_3 will play the role of decision maker, as denoted by $\mathfrak{D}_1$. Assume that the ratio of the discharging and recharging rate is $\alpha = 2$. This implies that each cycle T consists of 3 time slots. By applying the scheduling operations designed in this task, the scheduling result for g_1^{best} is shown in Fig. 7. In the beginning, the detection probability of g_1^{best} at each time slot is zero because that there is no sensor activated. The earliest time slot t_1 will be treated as the t_1^{bott}. In the first round, the decision maker $\mathfrak{D}_1$ schedules s_3 to be activated at t_1. In the second round, t_2 becomes the new bottleneck time slot and sensor s_4 has the largest contribution to g_1^{best} at time slot t_2. Therefore, $\mathfrak{D}_1$ schedules sensor s_4 to be activated at t_2. Finally, the scheduling result for g_1^{best} is given in the scheduling matrix $\mathcal{M}^{g_1^{best}}$ as shown in Fig. 7. As shown in this matrix, each scheduled sensor will be activated in one time slot and be recharged in two time slots. For example, as shown in the first column of $\mathcal{M}^{g_1^{best}}$, only sensor s_3 stays in sensing state. All the other sensors stay in recharging state. As shown in the second column of the $\mathcal{M}^{g_1^{best}}$, sensors s_1 and s_2 stay in sensing states. The sensing probability of the space time point $(g_1^{best}, 2)$ is

$$p_{1,2}^{best} = 1 - \left[1 - p\left(s_1, g_{(1,2)}\right)\right] \times \left[1 - p\left(s_2, g_{(1,2)}\right)\right] = 0.828$$

Similarly, as shown in the third column of $\mathcal{M}^{g_1^{best}}$, sensors s_4, s_5 and s_6 stay in sensing state. Therefore, the cooperative sensing probability is $p_{1,3}^{best} = 0.807$.

Task V (Selecting the Next Best Grid): Herein, we notice that the barrier is constructed from left boundary to right boundary by repeatedly selecting the best grid. Therefore, the proposed *MCDP* algorithm selects the best grid at a time and connects the selected best grid to the already constructed barrier. As soon as the scheduling operation for the first best grid has been accomplished, the next major work of this task is to select the next best grid for extending the length of the constructed barrier. To achieve this, the next best grid should be selected from the right neighboring grids of the current best grid. The following defines the right neighboring grids of $g_{(l,k)}$. The grid $g_{(m,n)}$ is said to be the right neighboring grid of $g_{(l,k)}$ if it satisfies Exp. (32).

$$m - l = 1 \;\&\&\; |n - k| \leq 1 \tag{32}$$

Let $N_r\left(g_{(x,y)}\right) = \{g_1^{N_r}, g_2^{N_r}, \ldots, g_{|N_r(g_{(x,y)})|}^{N_r}\}$ denote the set of right neighboring grids of $g_{(x,y)}$. Assume the current best grid is g_i^{best}. Each grid $g_k^{N_r}$ in $N_r(g_i^{best})$ will be the candidate of next best grid. Since the scheduling operation for g_i^{best} has been accomplished, some scheduled sensors for monitoring g_i^{best} may also have contribution to the grids in $N_r(g_i^{best})$. Let $p_{k,h}^{N_r}$ denote the cooperative detection probability of space time point $(g_k^{N_r}, h)$, which is contributed by those already selected sensors. The $g_k^{N_r}$ which takes maximal advantages, in terms of detection probability, from the already selected sensors will be selected as the best grid. Recall q_i denotes the surveillance quality of g_i^{best}. Exp. (33) reflects the above mentioned condition.

$$g_{i+1}^{best} = \arg \underset{g_k^{N_r} \in N_r(g_i^{best})}{max} \sum_{h=1}^{\sigma} (p_{k,h}^{N_r} - q_i) \tag{33}$$

In case that there is no scheduled sensor contributed to any grid in $N_r(g_i^{best})$, the upper grid in $N_r(g_i^{best})$ will be selected as the next best one. This is because that the *MCDP* algorithm aims to utilize the unscheduled sensors from top to bottom.

Fig. 6 continuously gives an example to illustrate the operations for selecting the next best grid. Assume that grid $g_{(1,2)}$ has been selected as the first best grid. The set of candidates of the second best grids is

$$N_r\left(g_1^{best}\right) = \{g_1^{N_r}, g_2^{N_r}, g_3^{N_r}\}$$

which are marked with read shadow color. The table in Fig. 6 gives the contribution of each scheduled sensor to each space time point $(g_k^{N_r}, h)$, where $g_k^{N_r} \in N_r(g_1^{best})$. By applying Exp. (33), the detection probability of $g_2^{N_r}$ is selected as the best grid g_2^{best}. Meanwhile, sensor s_2 will play the role of $\mathfrak{D}_2$ because it is the closest sensor to the central point of g_2^{best}. Then the operation of *Tasks III* and *IV* will be executed for g_2^{best}. The *next best grid selection operation* will be finished if the rightmost best grid which reaches the right boundary is selected.

Fig. 8 summaries the process of the *MCDP* algorithm. Steps 1 and 2 summarize the space-time partitioning phase. Then steps 3 and 4 summarize the computation phase. Finally, step 5 to step 9 summarize the barrier construction and sensor scheduling phase.

V. Simulation

This section studies the performance improvement of the proposed *MCDP* algorithm against the existing Best-fit Coverage Approach (*BCA*) and Top-down One-coverage Barrier Approach (*TOBA*) [14]. The *BCA* algorithm aimed to find the maximal number of disjoint k-barrier which consists of

The *MCDP* algorithm

Inputs:
1. A set of sensors $S = \{s_1, s_2, \ldots, s_n\}$ randomly deployed in *R*.
2. The physical location (x_i, y_i) of each deployed sensor s_i.
3. Parameters: E_{min}, E_{max}, u_{sen} and u_{rec}

Outputs: A set of active sensors which construct the barrier

Step 1. /* ***Space Partitioning*** */
Partition the R into $c_1 \times c_2$ equal-sized grids;
Step 2. /* ***Time Partitioning Phase*** */
$\tau = t_{sen} = \frac{E_{max}-E_{min}}{u_{sen}}$
Step 3. /* ***Cycle Length Calculation*** */
$T = t_{sen} + t_{rec} = (\alpha + 1)\tau$
Step 4. /* ***Detection probability Calculation*** */
If (grid $g_{(x,y)}$ is fully covered by sensor s_i)
Calculates $p(s_i, g_{(x,y)})$ according to Exp. (23)
else if (grid $g_{(x,y)}$ is covered by the set of sensors $\Phi_{(x,y)}$)
Calculates $p(\Phi_{(x,y)}, g_{(x,y)})$ according to Exp. (24)
Step 5. /* ***Group Sensor Partitioning*** */
For (each sensor $s_i \in S$)
{s_i is grouped into *j*-th group if it is located in the *j*-th sub-region;}
Step 6. /* ***Selecting the first best grid*** */
For (each group *j*) {
Identify g_1^{best} from candidates $g_{(1,y)}$.
Identify closest sensor to the central point of g_1^{best} to be $\mathfrak{D}_1$}
Repeat {
Step 7. /* ***Identifying of the Bottleneck Space Time Point****/
$t_1^{bott} = arg \min_{1 \le t_h \le \sigma} p_{1,h}^{best}$
Step 8. /* ***Scheduling Sensor for "Bottleneck"*** */
Repeat {
For (each $s_i \in S_{1,*}^{unsch}$) {
If (s_i satisfies Exp. (28))
{ $S_1^{opt} = S_1^{opt} \cup \{s_i\}$ }
If ($|S_1^{opt}| = 1$) {
$s^{opt} = s_i$
Else If ($|S_{c1}^{opt}| > 1$) {
Identify s^{opt} by applying Exp. (29)
Construct S_1^{opt} by $S_1^{opt} = S_1^{opt} s^{opt}$
Else If ($|S_1^{opt}| > 1$)
Randomly select one sensor in S_1^{opt} as the s^{opt};
Until q_i is maximized;
Step 9. /****Selecting the Next Best Grid*** */
For (each grid $g_k^{N_r} \in N_r(g_i^{best})$) {
$p_{k,h}^{N_r} - q_i$}
If ($g_k^{N_r}$ satisfies Exp. (33))
$g_k^{N_r}$ is g_{i+1}^{best};
Else If
$g_{i+1}^{best} = arg \min_{g_k^{N_r} \in N_r(g_i^{best})} y_k$
Executing the operations in Step 7 and Step 8; }
Until ($g_{rightmost}^{best} \cap B_{rightmost} \neq \emptyset$)

Fig. 8. The process of the *MCDP* algorithm.

the minimal number of active sensors. The *TOBA* algorithm aimed to find the maximal number of disjoint 1-barrier and form a *k*-barrier by integrating multiple 1-barrier. Both of the two algorithms are decentralized and are designed based on the grid-based method aiming at achieving the goals of energy balance and maximal lifetime. Herein, we notice that the proposed *MCDP* algorithm adopts the solar-power sensors which need to be recharged in every cycle. Though this can achieve the perpetual network lifetime of the considered WSNs, the coverage will be reduced when some sensors are recharging in the recharging slots. Therefore, it is not fair to compare the network lifetime of the WSNs or the energy consumptions of the sensors. In the experiments, the three

TABLE II
SIMULATION PARAMETER

Parameter	Value
Monitoring Region	800m×400m
Density Degree	1-5
Sensing Radius	10m-30m
Communication Radius	Twice of sensing radius
Grid Size	10m×10m
Deployment Strategy	Randomly/Uniformly
Ratio of the discharging and recharging rate	3

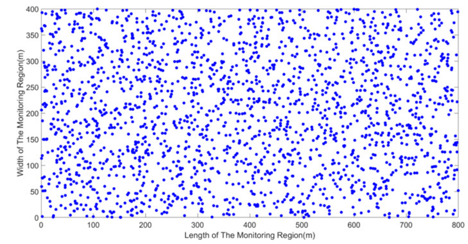

(a) A scenario that sensors are randomly deployed in the monitoring area.

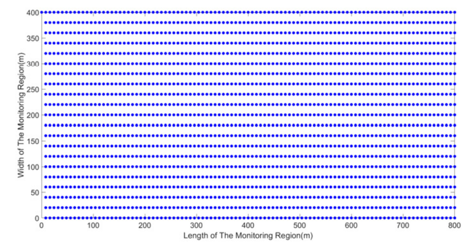

(b) A scenario that sensors are uniformly deployed in the monitoring area.

Fig. 9. The example of deployments where the random and uniform deployment strategies are applied in the monitoring region sized 800m*400m.

algorithms are compared in terms of the surveillance quality, the stability of cooperative detection probability as well as the fault tolerance capability. To fairly compare the three algorithms, the number of working sensors in each slot is set as a constant value. The following firstly illustrates the simulation model. Then the simulation results are presented.

A. Simulation Environment

The simulation parameters are given in Table II. As shown in Fig. 9, there are two sensor deployment scenarios. The first one is random deployment while the second one is uniform deployment. The size of the monitoring region is $800m \times 400m$. Herein, we define the *density degree* which represents the number of sensors covering each grid. In the experiment, the *density degree* is used to represent the density of the deployed sensors and its value is ranging from 1 to 5. The communication radius is twice of the sensing radius which is ranging from 10m to 30m. The grid size is set at 10m×10m. The ratio of the discharging and recharging rate is 3, and the cycle length is 4 time slots.

B. Simulation Results

Fig. 10 compares the surveillance quality by varying the sensing radius of each sensor and the density degree.

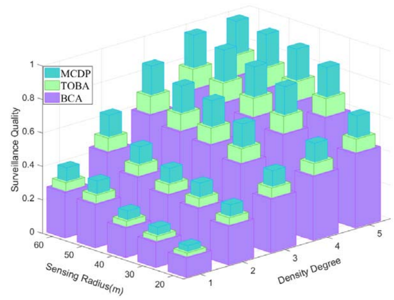

(a) The random deployment.

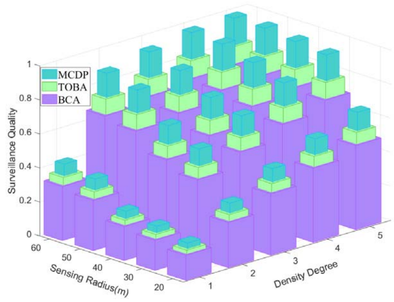

(b) The uniform deployment.

Fig. 10. Comparisons of *MCDP*, *TOBA* and *BCA* in terms of the surveillance quality by considering different sensing ranges and varying the density degree.

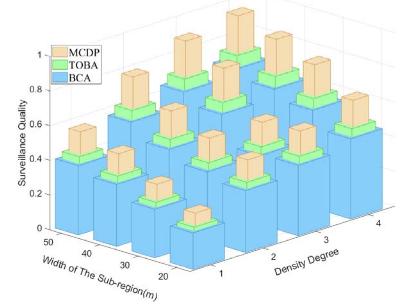

(a) The random deployment.

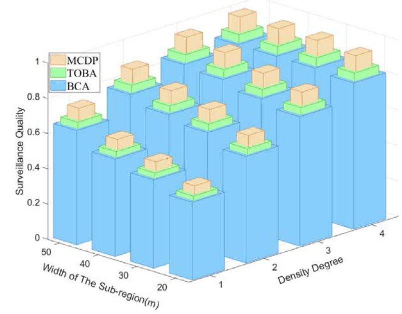

(b) The uniform deployment.

Fig. 11. Comparisons of *MCDP*, *TOBA* and *BCA* in terms of the surveillance quality by varying the width of the sub-region and the density degree.

In general, three compared algorithms have a similar trend in both random and uniform deployment strategies that the surveillance quality significantly increases with both the density degree and the sensing radius of each sensor. This occurs because more sensors can participate in monitoring task at each time slot if the sensors deployed in a higher density degree. Besides, a large sensing radius leads to a large coverage area, increasing the detection probability. In comparison, the uniform deployment strategy obtains a better result than random deployment. This occurs because that sensors deployed by applying the uniform deployment strategy can provide a better balanced detection probability. In comparison, the proposed *MCDP* algorithm outperforms the other two algorithms in terms of surveillance quality. This occurs because that the proposed *MCDP* applies *PSM* and selects the sensor with the largest contribution to each bottleneck space time point. Both *TOBA* and *BCA* algorithms aimed to construct a k-barrier with the minimal number of active sensors. Therefore, the selected sensors might not have the largest contribution to the bottleneck space time point. As a result, the performance of the *MCDP* algorithm outperforms the other two algorithms.

Fig. 11 investigates the surveillance quality by varying the width of the sub-region and density degree. The comparison results by applying random and uniform deployment strategies are shown in Figs. 11 (a) and 11 (b), respectively. As shown in Fig. 11, the surveillance qualities of three compared algorithms are generally increased with the width of the sub-region in both random and uniform deployment strategies. This occurs because that the larger width of the sub-region can provide more sensors to be scheduled for monitoring each best grid. Similar to the results obtained in Fig. 10, the uniform deployment strategy obtains a better result than the random deployment one. The performance of the proposed *MCDP* algorithm is better than those of *TOBA* and *BCA* algorithms. This occurs because that *TOBA* and *BCA* algorithms aimed to reduce both the computation complexity and the number of active sensors. Hence there are more constraints for selecting the active sensors.

Fig. 12 further studies the cooperative detection probability of randomly selected 9 points on the defense barrier. Fig. 12 (a) shows the cooperative detection probability of 9 points by applying the proposed *MCDP* at four time slots of one cycle. As shown in Fig. 12 (a), the cooperative detection probabilities of the selected point at four time slots are similar. It implies that the proposed *MCDP* algorithm supports good stability of cooperative detection probability. This occurs because that the *MCDP* algorithm identifies the bottleneck space time point and tries to schedule the sensor which has the largest contribution to the bottleneck space time point to be active. Therefore, the proposed *MCDP* can support better stability of cooperative detection probability, as compared with the other two algorithms. Fig. 12 (b) further compares the surveillance quality of 9 points by applying *MCDP*, *TOBA* and *BCA* algorithms. The observed locations are identical to those of Fig. 12 (a). The performance of the proposed *MCDP* algorithm is better than the existing *TOBA* and *BCA* algorithms in terms of the surveillance quality and its stability.

Fig. 13 further investigates the stability of the cooperative detection probability of each space time point on defense barrier. The observation locations are identical to those as

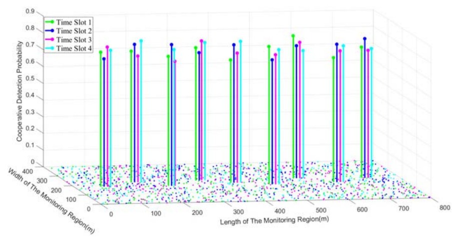

(a) Cooperative detection probability of *MDCP* in different time slots.

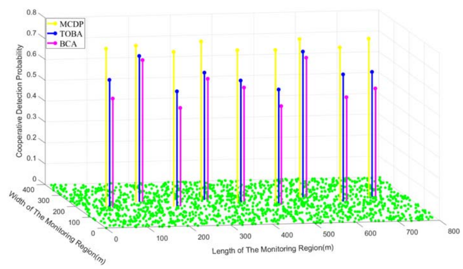

(b) Comparison of three algorithms in terms of cooperative detection probability.

Fig. 12. Comparison of cooperative detection probabilities of randomly selecting points.

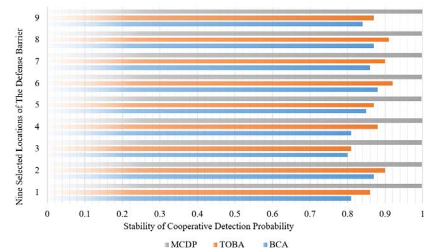

(a) Stability of each observed location.

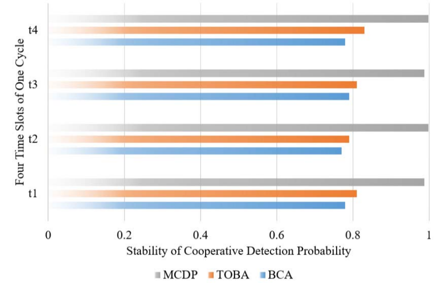

(b) Stability of each time slot.

Fig. 13. Comparison of the cooperative detection probability stability.

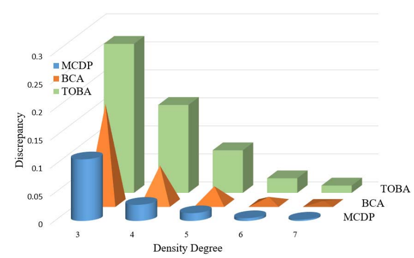

(a) The random deployment.

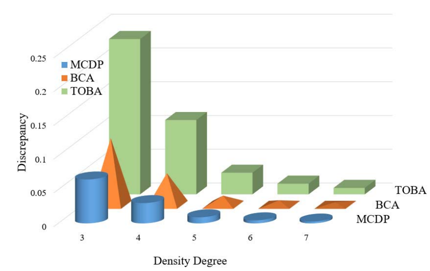

(b) The uniform deployment.

Fig. 14. Comparisons of *MCDP*, *TOBA* and *BCA* in terms of fault tolerance by varying the density degree.

shown in Fig. 12. The stability of cooperative detection probability can be measured by different degrees of cooperative detection probability for a given σ time slots or a given m locations. Recall that $p_{i,h}$ denotes the cooperative detection probability of the i-th location at the h-th time slot. The stability of the i-th location for σ time slots and the stability of the h-th time slot on m locations are defined by δ_i and δ_h, respectively. That is,

$$\delta_i = \frac{(\sum_{h=1}^{\sigma} p_{i,h})^2}{\sigma \sum_{h=1}^{\sigma} (p_{i,h})^2} \tag{34}$$

$$\delta_h = \frac{(\sum_{i=1}^{m} p_{i,h})^2}{m \sum_{i=1}^{m} (p_{i,h})^2} \tag{35}$$

Fig. 13 (a) first compares the stabilities of four time slots on nine locations. The value of stability approaching to 1 indicates that the cooperative detection probabilities of m locations are similar. The proposed *MCDP* algorithm outperforms the other two existing algorithms in terms of stability and approaches to 1 for all observed locations. This occurs because that the *MCDP* algorithm prior schedules the sensor which has the largest detection probability contribution to the bottleneck space time point. Fig. 13 (b) further compares the stability of nine locations at four time slots. The results are similar to those as shown in Fig. 13 (a). The proposed *MCDP* algorithm outperforms the other two compared algorithms in terms the stability of each time slot for the defense barrier.

Fig. 14 compares the fault tolerance capability of three compared algorithms by varying the density degree, which can be measured by the discrepancy of cooperative detection probability if some sensor is broken. Recall that $S_{i,h}^{sch}$ denotes the set of sensors which has been scheduled for monitoring grid g_i^{best} at time slot t_h. Let $S_{i,h}^{fail}$ denote the set of failure sensors in $S_{i,h}^{sch}$. Let $\Theta_{S_{i,h}^{dis}}$ denote the discrepancy of cooperative detection probability if some sensors in $S_{i,h}^{sch}$ suddenly broken. The value of $\Theta_{S_{i,h}^{fail}}$ can be calculated by Exp. (36)

$$\Theta_{S_{i,h}^{dis}} = \frac{p^{coop}\left(S_{i,h}^{sch}, g_i^{best}\right) - p^{coop}\left(S_{i,h}^{sch} \setminus S_{i,h}^{fail}, g_i^{best}\right)}{p^{coop}\left(S_{i,h}^{sch}, g_i^{best}\right)} \tag{36}$$

The value of $\Theta_{S_{i,h}^{dis}}$ approaching to 0 implies that the corresponding algorithm has better fault tolerance capability. Because that surveillance quality is determined by the cooperative detection probability at the bottleneck space time point. Fig. 14 (a) compares the fault tolerance capability of barrier if one sensor monitoring the bottleneck space time point is failure. As shown in Fig. 14 (a), the fault tolerance capability of the proposed *MCDP* is better than those of the existing *TOBA* and *BCA* algorithms. This occurs because the *MCDP* aims to find the sensors which are able to cooperative monitor every location on the barrier. However, the other two algorithms aimed to guarantee the coverage degree without considering the detection probability. Therefore, the impact on surveillance quality of the barrier constructed by *MCDP* is relatively small if one active sensor is failure. Fig. 14 (b) shows a similar result though it adopts uniform deployment strategy.

VI. Conclusion

This paper proposes a barrier coverage algorithm, called *MCDP*, which applies *PSM* sensing model and aims to perpetuate the lifetime of solar-powered WSNs while maximizing the surveillance quality of the constructed barrier. In order to perpetuate the lifetime of the solar-powered WSNs, each sensor is scheduled to stay in recharging and sensing states in different time slots. To maximize the surveillance quality of the constructed barrier, the proposed *MCDP* algorithm first calculates the detection probability of each sensor to each grid. Then it selects the best grid from the left boundary to the right boundary and schedules the sensor with the largest contribution to the bottleneck space time point. Extensive simulations demonstrate that the proposed *MCDP* algorithm outperforms the compared *TOBA* and *BCA* algorithms in terms of surveillance quality, the stability of cooperative detection probability as well as the fault tolerance capability. Future work will consider solar-powered sensor with adjustable sensing radius and further optimize the surveillance quality for each space time point.

References

[1] C.-F. Cheng and C.-W. Wang, "The Barrier-breach problem of Barrier coverage in wireless sensor networks," *IEEE Commun. Lett.*, vol. 21, no. 10, pp. 2262–2265, Oct. 2017.

[2] Y. Wang, S. Wu, Z. Chen, X. Gao, and G. Chen, "Coverage problem with uncertain properties in wireless sensor networks: A survey," *Comput. Netw.*, vol. 123, pp. 200–232, Aug. 2017.

[3] C.-F. Cheng and C.-W. Wang, "The target-Barrier coverage problem in wireless sensor networks," *IEEE Trans. Mobile Comput.*, vol. 17, no. 5, pp. 1216–1232, May 2018.

[4] Y. Chen, S. Huang, and R. Fitch, "Active SLAM for mobile robots with area coverage and obstacle avoidance," *IEEE/ASME Trans. Mechatronics*, vol. 25, no. 3, pp. 1182–1192, Jun. 2020.

[5] H. Mostafaei, M. U. Chowdhury, and M. S. Obaidat, "Border surveillance with WSN systems in a distributed manner," *IEEE Syst. J.*, vol. 12, no. 4, pp. 3703–3712, Dec. 2018.

[6] H. M. Ammari, "Investigating physical security in stealthy lattice wireless sensor networks using k-Barrier coverage," *Ad Hoc Netw.*, vol. 89, pp. 142–160, Jun. 2019.

[7] Z. Wang, H. Chen, Q. Cao, H. Qi, Z. Wang, and Q. Wang, "Achieving location error tolerant Barrier coverage for wireless sensor networks," *Comput. Netw.*, vol. 112, pp. 314–328, Jan. 2017.

[8] X. Zhang, Y. Zhou, Q. Zhang, V. C. S. Lee, and M. Li, "Problem specific MOEA/D for Barrier coverage with wireless sensors," *IEEE Trans. Cybern.*, vol. 47, no. 11, pp. 3854–3865, Nov. 2017.

[9] J. Yu, S. Wan, X. Cheng, and D. Yu, "Coverage contribution area based k-coverage for wireless sensor networks," *IEEE Trans. Veh. Technol.*, vol. 66, no. 9, pp. 8510–8523, Sep. 2017.

[10] C.-Y. Chang, Y.-W. Kuo, P. Xu, and H. Chen, "Monitoring quality guaranteed Barrier coverage mechanism for traffic counting in wireless sensor networks," *IEEE Access*, vol. 6, pp. 30778–30792, 2018.

[11] D. Thomas, R. Shankaran, M. Orgun, M. Hitchens, and W. Ni, "Energy-efficient military surveillance: Coverage meets connectivity," *IEEE Sensors J.*, vol. 19, no. 10, pp. 3902–3911, May 2019.

[12] B. Khalifa, Z. A. Aghbari, A. M. Khedr, and J. H. Abawajy, "Coverage hole repair in WSNs using cascaded neighbor intervention," *IEEE Sensors J.*, vol. 17, no. 21, pp. 7209–7216, Nov. 2017.

[13] C. Qiu, H. Shen, and K. Chen, "An energy-efficient and distributed cooperation mechanism for k-coverage hole detection and healing in WSNs," *IEEE Trans. Mobile Comput.*, vol. 17, no. 6, pp. 1247–1259, Jun. 2018.

[14] C.-I Weng; C.-Y. Chang, C.-Y. Hsiao, C. -T. Chang, and H. Chen, "On-supporting energy balanced k-Barrier coverage in wireless sensor networks," *IEEE Access*, vol. 6 pp. 13261–13274, 2018.

[15] D. Kim, W. Wang, J. Son, W. Wu, W. Lee, and A. O. Tokuta, "Maximum lifetime combined Barrier-coverage of weak static sensors and strong mobile sensors," *IEEE Trans. Mobile Comput.*, vol. 16, no. 7, pp. 1956–1966, Jul. 2017.

[16] Z. Zhang, J. Willson, Z. Lu, W. Wu, X. Zhu, and D.-Z. Du, "Approximating maximum lifetime k-coverage through minimizing weighted k-cover in homogeneous wireless sensor networks," *IEEE/ACM Trans. Netw.*, vol. 24, no. 6, pp. 3620–3633, Dec. 2016.

[17] S. Silvestri and K. Goss, "MobiBar: An autonomous deployment algorithm for Barrier coverage with mobile sensors," *Ad Hoc Netw.*, vol. 54, pp. 111–129, Jan. 2017.

[18] L. Kong *et al.*, "Adaptive Barrier coverage using software defined sensor networks," *IEEE Sensors J.*, vol. 16, no. 20, pp. 7364–7372, Oct. 2016.

[19] X. Zhang, M. L. Wymore, D. Qiao, "An iterative method for strong Barrier coverage under practical constraints," in *Proc. IEEE Int. Conf. Commun. (ICC)*, May 2016, pp. 1–7.

[20] J. Chen, J. Li, and T. H. Lai, "Energy-efficient intrusion detection with a Barrier of probabilistic sensors: Global and local," *IEEE Trans. Wireless Commun.*, vol. 12, no. 9, pp. 4742–4755, Sep. 2013.

[21] H. P. Gupta, S. V. Rao, and T. Venkatesh, "Sleep scheduling protocol for k-coverage of three-dimensional heterogeneous WSNs," *IEEE Trans. Veh. Technol.*, vol. 65, no. 10, pp. 8423–8431, Oct. 2016.

[22] Z. Zhang, W. Wu, J. Yuan, and D.-Z. Du, "Breach-free sleep-wakeup scheduling for Barrier coverage with heterogeneous wireless sensors," *IEEE/ACM Trans. Netw.*, vol. 26, no. 5, pp. 2404–2413, Oct. 2018.

[23] N. Aslam, K. Xia, and M. U. Hadi, "Optimal wireless charging inclusive of intellectual routing based on SARSA learning in renewable wireless sensor networks," *IEEE Sensors J.*, vol. 19, no. 18, pp. 8340–8351, Sep. 2019.

[24] H. Chen, X. Li, and F. Zhao, "A reinforcement learning-based sleep scheduling algorithm for desired area coverage in solar-powered wireless sensor networks," *IEEE Sensors J.*, vol. 16, no. 8, pp. 2763–2774, Apr. 2016.

[25] D. Arivudainambi and S. Balaji, "Optimal placement of wireless chargers in rechargeable sensor networks," *IEEE Sensors J.*, vol. 18, no. 10, pp. 4212–4222, May 2018.